

## Films Made from Poly(vinyl alcohol-co-ethylene) and Soluble Biopolymers Isolated from Municipal Biowaste

Flavia Franzoso,<sup>1</sup> Silvia Tabasso,<sup>1</sup> Diego Antonioli,<sup>2</sup> Enzo Montoneri,<sup>3</sup>  
Paola Persico,<sup>4</sup> Michele Laus,<sup>2</sup> Raniero Mendichi,<sup>4</sup> Michele Negre<sup>5</sup>

<sup>1</sup>Dipartimento di Chimica, Università di Torino, Via P. Giuria 7, 10125 Turin, Italy

<sup>2</sup>Dipartimento di Scienze e Innovazione Tecnologica, Università degli Studi del Piemonte Orientale A. Avogadro, Italian Interuniversity Consortium for Materials Science and Technology (INSTM), Research Unit Alessandria, Viale T. Michel 11, 15121 Alessandria, Italy

<sup>3</sup>STAR Integrated Research Unit, Università di Foggia, Via Gramsci 89-91, 71121 Foggia, Italy

<sup>4</sup>Istituto per lo Studio delle Macromolecole, Via E. Bassini 15, 20133 Milan, Italy

<sup>5</sup>Dipartimento di Scienze Agrarie, Forestali e Alimentari, Università di Torino, Via L. da Vinci 44, 10095 Turin, Italy

Correspondence to: E. Montoneri (E-mail: enzo.montoneri@gmail.com)

**ABSTRACT:** Blends were obtained from poly(vinyl alcohol-co-ethylene) and water-soluble biopolymers isolated from the alkaline hydrolysate of two materials sampled from an urban waste treatment plant: that is, an anaerobic fermentation digestate and a compost. The digestate biopolymers contained more lipophilic and aliphatic C and less acidic functional groups than the compost biopolymers. Evidence was obtained for a condensation reaction occurring between the biopolymers and the synthetic polymer. The thermal, rheological, and mechanical properties of the blends were studied. Films containing a low concentration (ca. 6–7%) of biopolymers exhibited up to three times higher yield strength than the neat synthetic polymer. The films' properties were found to be dependent on the concentration and nature of the biopolymers. The results offer a scope for investigating biopolymers sourced from other biowastes and for a better understanding of the reasons for the observed effects and exploiting their full potential for modifying or replacing synthetic polymers. © 2014 Wiley Periodicals, Inc. *J. Appl. Polym. Sci.* **2015**, *132*, 41359.

**KEYWORDS:** biopolymers and renewable polymers; blends; copolymers; films; mechanical properties

Received 23 March 2014; accepted 28 July 2014

DOI: 10.1002/app.41359

### INTRODUCTION

Soluble bioorganic substances (SBOs)<sup>1</sup> obtained by the alkaline hydrolysis of fermented urban residues are complex mixtures of molecules with weight-average molar masses ( $M_w$ 's) of 67–463 kg/mol. These products contain acid and basic functional groups bonded to aromatic (Ph) and aliphatic (Af) C chains. In solution, they behave like small-molecule surfactants and are capable of enhancing the water solubility of lipophilic molecules and complex metal ions. Because of these properties, they represent promising chemical auxiliaries for a large number of applications in chemical industries, environmental technology, agriculture, and animal husbandry. The polymeric nature of these products suggest that they could also be used for the manufacture of articles that are nowadays made from synthetic polymers from fossil sources. SBOs, however, decompose at about 220°C without melting and do not have film-forming properties. They are only soluble in water at pH values greater than 4. The evaporation of their water solutions results in the

deposition of the solute in powder or fragile sheet form. Thus, neat SBO cannot be processed to obtain usable objects. Under these circumstances, the only possibility is compounding them with other polymeric materials to obtain processable blends.

Blends of synthetic polymers and biopolymers of agricultural sources are well known. Several blends of poly(vinyl alcohol) (PVA), vinyl alcohol-ethylene copolymers (EVOHs), and polysaccharides, such as starch<sup>2–4</sup> or lignocellulosic materials including corn fiber<sup>5</sup> and sugar cane bagasse,<sup>6–9</sup> have been reported. These products have been proposed for the manufacturing of mulch films for use in agriculture. In these films, the synthetic polymer provides the required mechanical properties and is compatible with the lignocellulosic fillers by virtue of its hydroxyl and carboxyl groups. To our knowledge, blend materials containing SBOs or similar lignocellulosic hydrolysates obtained from any other source have not been reported so far. PVA-based blends containing SBOs are attractive for several reasons. First, these blends would benefit from the hydrophilic

functional groups of SBOs and from the mechanical properties contributed by the synthetic polymer. Thus, new ion-exchange membranes or hydrophilic films for diversified uses could be obtained. Second, the use of SBOs for manufacturing articles enlarges the perspectives to recycle SBOs in chemical industry. This makes biowastes promising as source of added-value products and, therefore, opens new scenarios for the cost-effective ecofriendly management of urban wastes. Third, SBOs are sourced from negative-cost<sup>10</sup> refuse materials, which are available in concentrated form in all urban contexts throughout the world, and not from dedicated crop or agriculture residues scattered over large areas. Fourth, the production cost of SBOs, estimated<sup>11</sup> to be 0.1–0.5 €/kg, is much lower than the cost of EVOH. Thus, the partial substitution of synthetic polymers with SBOs would imply a significant reduction in the cost impact of the starting components in the finished film product.

In this article, we report the preparation and chemical, molecular, thermal, and mechanical characterization of EVOH films containing various amounts of two different types of SBOs. These biopolymers were sourced from two different urban biowastes, which represented the major effluents of modern municipal waste management plants, that is, a digestate of the anaerobic degradation of an organic humid fraction (FORSUD) and the compost (CVDF) obtained from a mix of home garden and public park trimmings, digestate, and sewage sludge. According to their different sources, the two SBOs were significantly different in their types and levels of hydrophilicity. The availability of these products allowed us to investigate EVOH–SBO films as a function of their biopolymer concentration and chemical nature.

## EXPERIMENTAL

### Materials

The SBOs were sourced from municipal biowastes sampled from two different streams of the ACEA Pinerolese waste treatment plant in Pinerolo, Italy. These were the digestate (FORSUD) recovered from the plant biogas production reactor fed with the organic humid fraction from a separate source collection of urban refuse and the compost (CVDF) obtained from a 35/55/10 w/w/w FORSUD/home gardening and a park trimming residue/sewage sludge mix composted for 110 days. These materials were processed in a pilot plant made available from Studio Chiono e Associati in Rivarolo (Canavese, Italy). The pilot plant was composed of an electrically heated mechanically stirred 500-L reactor, a 102 cm long × 10.1 cm diameter polysulfone ultrafiltration membrane with a 5-kDa molar mass cutoff supplied by Idea Engineering s.r.l. from Lessona (Bi, Italy), and a forced-ventilation drying oven. According to the experimental operating conditions, the FORSUD or CVDF was reacted for 4 h with pH 13 aqueous KOH at 60°C and with a 4 v/w liquid/solid ratio. The liquid/solid mix was allowed to settle to separate the supernatant liquid phase containing the soluble hydrolysate from the insoluble residue. The recovered hydrolysate was circulated at a 40 L/h flow rate through a 5-kDa cutoff polysulfone ultrafiltration membrane operating with a tangential flow at a 7-bar inlet and a 4.5-bar outlet pressure to yield a retentate with a 5–10% dry matter content. The concentrated retentate was finally dried at 60°C to yield the solid

SBO as a black powder in 15–30 wt % yield, relative to the starting biowaste dry matter. The SBOs are hereinafter referred to with the acronym of the sourcing biowaste. These products were found to contain about 15–28 wt % ash. The ash contained, along with the added alkali cation of the hydrolyzing base, other mineral elements present in the sourcing biowaste, including Si, Ca, Mg, Al, and Fe. The products were characterized for their C types and functional group content through a combination of the analytical data obtained by <sup>13</sup>C-NMR spectroscopy, potentiometric titration, and microanalysis and were obtained according to previously reported details.<sup>1</sup> Pellets of EVOH (PVA-co-ethylene with 38 mol % ethylene, commercial name Soarnol, CAS number 26221-27-2) were supplied by Nippon Gohsei Europe GmbH (Düsseldorf). Dimethyl sulfoxide (DMSO; CAS number 67-68-5) was supplied by Sigma Aldrich and was used as purchased.

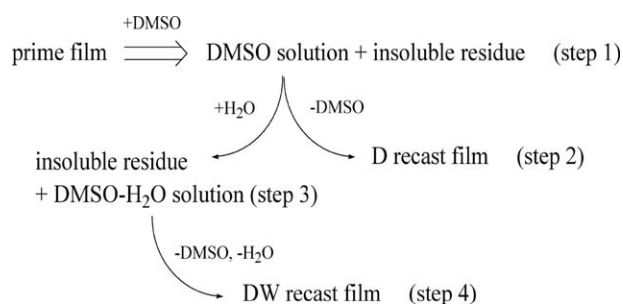
### Preparation of the EVOH–SBO Films

The EVOH pellets (10 g) were dissolved in 100 mL of DMSO under stirring at 120°C. The SBO samples (100 g) were dissolved in 1 L of water under stirring for 2 h at room temperature. Then, an appropriate amount of SBO solution was added dropwise to the hot EVOH solution to allow water distillation and to obtain a final homogeneous solution containing the desired amounts of EVOH and SBOs. Several samples were obtained according to the previous general procedure by the variation of the initial SBO amount. The heating of this solution was continued to complete the removal of the residual water added with SBOs, as measured by the collected volume of the distilled water. The solution was then heated *in vacuo* to evaporate DMSO. The solvent evaporation was continued to obtain a viscous flowing liquid that could be poured and spread on a hot casting plate by a doctor blade moving along the stationary casting surface. The resulting viscous wet layer was heated at 105°C overnight on a hot plate to yield a film coating the casting plate surface. The assembly was then immersed in a water bath for at least 1 h to allow film detachment from the plate surface. During this operation, the water bath became colored by the release of the unreacted SBO (see the Results and Discussion section). The recovered freestanding film was washed again with water to remove the residual DMSO and unreacted SBO. This operation was repeated until the final collected water washing was colorless. Films 150 μm in thickness were typically obtained. The films were obtained from DMSO solutions containing SBO and EVOH in the 0.1–0.7 SBO/EVOH weight ratio range. Only products in powder form were obtained at an SBO/EVOH weight ratio greater than 0.7. Neat EVOH films were prepared by the same solvent casting procedure with the previous EVOH solution in DMSO without addition of SBOs. The films prepared according to this procedure are hereinafter referred to as the prime films.

### Product Fractionation Based on Solubility

Product fractionation was performed according to Scheme 1

In step 1, the prime film, thoroughly washed with water as described previously, was suspended in fresh DMSO at a 1/30 w/v ratio and heated 1 h at 120°C. The suspension was then centrifuged to separate the insoluble residue from the supernatant



**Scheme 1.** Solution-casting cycles of films containing EVOH and SBO with DMSO and DMSO-H<sub>2</sub>O as solvents.

DMSO solution. This solution was divided in two aliquots. One was cast as described previously for the prime film to yield the DMSO (D) recast film (step 2). The second aliquot was added with water at a 2.3 H<sub>2</sub>O/DMSO v/v ratio and centrifuged to separate any insoluble residue (step 3). The supernatant DMSO-H<sub>2</sub>O solution was cast as described previously to yield the DMSO/Water (DW) recast film (step 4). All fractions were weighed and analyzed for their chemical compositions.

#### Product Stability in 1M NaOH

The prime film was suspended in aqueous 1M NaOH at a 1/100 w/v ratio and kept 4 h at room temperature or heated 4 h at 60°C. The film was then withdrawn from the water phase, washed with water to pH 6, dried, weighed, and analyzed for its chemical composition. The water phase was acidified to test for the presence of any precipitated material. A similar treatment was performed on the products obtained from the Scheme 1 treatments, that is, the insoluble residue from steps 1 and 3 and the D and DW recast films from steps 2 and 4.

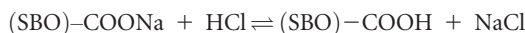
#### Determination of the Net Organic Matter (SBO<sub>nom</sub>) Contributed by SBOs in the EVOH-SBO Films

The organic fraction contributed by SBOs in the film was calculated on the basis of the N and carboxylic acid (COOH) analytical concentration values, according to eqs. (1) and (2).

$$\text{SBO}_{\text{nom}1} = N_f \times \text{VS}/N \quad (1)$$

$$\text{SBO}_{\text{nom}2} = \text{COOH}_f \times \text{VS}/\text{COOH} \quad (2)$$

where VS, N, and COOH are the volatile solid (wt %), elemental N (wt %), and COOH (mol/wt %) contents, respectively, in the neat SBO sample and  $N_f$  and  $\text{COOH}_f$  are the elemental N (wt %) and COOH (mol/wt %) contents, respectively, in the EVOH-SBO film. The COOH content in the neat SBO and the VS and N contents in the neat SBO samples and in the EVOH-SBO films were determined by potentiometric titration, calcination at 650°C, and microanalysis, respectively, according to previously reported procedures.<sup>1</sup> The potentiometric titration to determine the  $\text{COOH}_f$  in the EVOH-SBO films was performed on the basis of reaction 1 (the titration of carboxylate functional groups with HCl) as follows:



We confirmed the presence of carboxylate functional groups in the film by equilibrating the film with excess aqueous HCl,

withdrawing the film from the acid aqueous medium, washing it with water to pH 6, and drying it. The IR spectrum of the recovered film, compared to the IR spectrum of the starting film, showed that the starting film COONa absorption band centered at 1650 cm<sup>-1</sup> (see Results and Discussion section) was not picked out anymore in the film treated with HCl. However, the spectrum of this film exhibited a band centered at the typical absorption wavelength of COOH at 1710 cm<sup>-1</sup>. As the esterification of COONa during the reaction with EVOH was unlikely, we assumed that the COONa groups in the film indicated the total amount of SBO present in the film. The film sample was, therefore, first immersed and kept overnight under stirring in deionized water. A known volume of HCl 0.1M was added. The potential was measured after roughly 0.5 h after each addition. This time was necessary to allow the diffusion of the titrant in the film and to register the stable potential at equilibrium. For each film, a potential versus added HCl sigmoid curve was obtained. The volume of the tritrant needed to reach the inflection point of the curve was measured and used in eq. (2) to calculate SBO<sub>nom2</sub>.

#### Determination of the Amount of PVA-co-Ethylene copolymer (EVOH) with an Unaltered Melting Point (EVOH<sub>u</sub>) and Nonmelting EVOH (EVOH<sub>nm</sub>) in the EVOH-SBO Films

The EVOH<sub>u</sub> (w/w %) was determined from eq. (3):

$$\text{EVOH}_u = 100\Delta H_{\text{EVOH-SBO}}/\Delta H_{\text{EVOH}} \quad (3)$$

where  $\Delta H_{\text{EVOH-SBO}}$  and  $\Delta H_{\text{EVOH}}$  are the melting enthalpy values (J/g of VS) obtained by differential scanning calorimetry (DSC) of the EVOH film containing SBO and the neat EVOH film, respectively. The EVOH<sub>nm</sub> values were determined from eqs. (4) and (5):

$$\text{EVOH}_t = 100 - \text{SBO}_{\text{nom}} - \text{Ash} \quad (4)$$

$$\text{EVOH}_{nm} = \text{EVOH}_t - \text{EVOH}_u \quad (5)$$

where EVOH<sub>t</sub> is the total content (w/w %) of EVOH in the film, Ash is the percentage ash in the film dry matter as determined by calcinations of the film at 650°C, and SBO<sub>nom</sub> and EVOH<sub>u</sub> are the concentrations (w/w %) according to eqs. (1), (2), and (3).

#### Molar Mass Characterization of the EVOH-SBO Films

The molecular characterization of the neat SBO in powder form and of the neat EVOH and the EVOH-SBO films was performed with a multi-angle laser light scattering (MALLS) absolute detector online to a size exclusion chromatography (SEC) system. The molar mass distribution (MWD) was obtained by a modular multidetectors SEC system. The SEC system consisted of an Alliance 2695 separation module from Waters (Milford, MA) equipped with two online detectors: a MALLS Dawn DSP-F photometer from Wyatt (Santa Barbara, CA) and a 2414 Differential Refractometer Index (DRI) from Waters as concentration detector. The experimental methodology for the reliable use of the SEC-MALLS system has been described in the literature.<sup>12,13</sup> In detail, the SEC-MALLS chromatographic experimental conditions were as follows: for the neat EVOH and EVOH-SBO films, 2 PLgel Mixed C columns from Polymer Laboratories, dimethylacetamide plus 0.05M LiBr as the mobile phase, an 80°C temperature, an 0.8 mL/min flow rate, a 100- $\mu$ L

**Table I.** Chemical Compositions, Macromolecular Features, and  $\Delta H_m$  Values of the Neat SBO Powder, Neat EVOH, and EVOH–SBO Films

Sample	Composition (wt %) <sup>a</sup>			Molecular weight data			Mass recovery (w/w %) <sup>b</sup>	$\Delta H_m$ (J/g) <sup>c</sup>
	EVOH <sub>u</sub>	EVOH <sub>nm</sub>	SBO	$M_p$ (kD)	$M_w$ (kD)	$M_w/M_n$		
CVDF	—	—	67.6	61.5	75.1	1.53	88.5	
FORSUD	—	—	77.4	87.3	163.7	1.93	90.2	—
EVOH	99.2	—	—	24.6	31.5	2.23	97.2	64.0
EVOH–CVDF 6.2%	56.9	34.3	6.2	33.9	52.2	3.32	90.1	36.4
EVOH–CVDF 14.2%	38.1	42.8	14.2	43.6	59.3	2.71	82.6	24.4
EVOH–CVDF 18.9%	32.8	45.0	18.9	—	—	—	—	21.0
EVOH–FORSUD 5.9%	87.0	6.1	5.9	78.6	96.4	1.79	96.0	55.7
EVOH–FORSUD 9.9%	68.3	20.7	9.9	—	—	—	—	43.7
EVOH–FORSUD 8.7%	56.4	33.1	8.7	36.5	47.2	2.19	91.4	36.1

<sup>a</sup> Net ash-free organic matter contributed by EVOH<sub>u</sub>, EVOH<sub>nm</sub>, and SBO. Difference from 100 = ash content.

<sup>b</sup> Sample total mass recovery from SEC column.

<sup>c</sup>  $\Delta H_m$  with reference to the sample volatile solid unit weight.

injection volume, and about a 2 mg/mL sample concentration. For the neat SBO, the conditions were as follows: 2 Polar Gel (M and L) columns from Polymer Laboratories, 90% 0.1M carbonate buffer, pH 10.0 plus 10% methanol as the mobile phase, a 35°C temperature, a 0.8 mL/min flow rate, a 100- $\mu$ L injection volume, and about a 2 mg/mL sample concentration.

#### Other Measurements

Fourier transform infrared (FTIR) spectra were recorded in transmission mode in a PerkinElmer Spectrum BX spectrophotometer equipped with a Deuterated Triglycine Sulfate (DTGS) detector and working with 16 scans at a 4-cm<sup>-1</sup> resolution in the 4000–400-cm<sup>-1</sup> range. The FTIR analysis in transmission was carried out directly on the films or on KBr pellets for neat SBO. X-ray diffraction (XRD) patterns were obtained with a PW3040/60 X'Pert PRO MPD diffractometer from PANalytical in Bragg–Brentano geometry and equipped with a high-power ceramic tube PW3373/10 LFF source with a Cu anode. DSC was carried out with a Mettler-Toledo DSC 821<sup>e</sup> apparatus. Samples of about 5 mg were used. The instrument was calibrated with high-purity standards at 10°C/min. Dry nitrogen was used as the purge gas. The following temperature program was used: heating at 20°C/min from 25 to 200°C, then cooling at -10°C/min to 25°C, and finally heating again at 10°C/min to 200°C. Rheological tests were performed with an ARES strain-controlled rheometer (Rheometric Scientific). The frequency ( $\omega$ ) sweep tests were performed at a strain of 5.0% over a  $\omega$  range from 100 to 0.1 rad/s at 200°C with a parallel-plate geometry (diameter = 25 mm). A compressive constant force of 1.0N was applied to the samples during the measurements.<sup>14</sup> The mechanical tests were performed with a dynamical mechanical analyzer (DMTA V, Rheometric Scientific). All tests were carried out at a temperature of 25°C with the rectangular tension geometry on a specimen machined into bars with a size of 20 × 5 × 0.15 mm<sup>3</sup> with a gauge length of 10 mm. The stress-strain mechanical analysis was performed at a strain rate of 0.01 s<sup>-1</sup> with a preload force of 0.01 N. Five measurements were carried out on different specimens for each sample.<sup>15</sup>

## RESULTS AND DISCUSSION

### Chemical Nature of SBO

In this study, two different SBOs were used: FORSUD and CVDF. According to the details reported in the Experimental section, these products, sourced from biological materials of different origins, are hydrolysates containing organic matter with molar mass above 5 kD. Indeed, the SEC–MALLS data in Table I confirm that the two products contained macromolecules with  $M_w$ 's of 75 (CVDF) and 164 (FORSUD) kD.

Because of the nature of the sourcing materials, the chemical composition and structure of these macromolecules could not be characterized as precisely as those of the synthetic products. They should be viewed as complex mixtures of macromolecules differing in molecular weight and chemical nature. Analytical data for the whole molecular pool representing each SBO were obtained by microanalysis, potentiometric titration, and <sup>13</sup>C-NMR spectroscopy. These were elaborated according to a previously reported procedure<sup>1</sup> to yield the data reported in Table II for several C types and functional groups; that is, Af, Ph, methoxy (OMe), amide (CON), ammine (NR), alkoxy (RO), phenoxy (PhOY), anomeric (OCO), COOH, phenol (PhOH), and ketone (C=O) C atoms. These organic moieties were the likely memory of the main constituents of the sourcing waste digestate and compost bioorganic matter that were not completely mineralized during aging under fermentation conditions. The above C types and functional groups were likely to be inhomogeneously distributed over the entire molecular pool of each SBO. Notwithstanding these limitations in the chemical characterization, the available data allowed us to determine that the two products had different chemical features. Comparing the two SBOs for the values of each of the C atoms and functional groups reported in Table II was rather difficult. An easier and more meaningful way was by the following two parameters. One was the lipophilic to hydrophilic C ratio (LH) parameter, which is given by the ratio of the sum of the lipophilic Af, Ph, OMe, CON, NR, RO, PhOY, and OCO C atoms to the sum of the hydrophilic COOH, PhOH, and C=O C atoms. By this

**Table II.** Chemical Data for SBO Identified According to the Acronym of the Sourcing Biowaste (See the Experimental Section)

SBO	Ash (wt %) <sup>a</sup>	C (wt %) <sup>a</sup>		N (wt %) <sup>a</sup>		C/N							
FORSUD	22.6	42.90 ± 0.12		6.60 ± 0.12		6.5							
CVDF	32.4	36.70 ± 0.09		5.20 ± 0.17		7.1							
C Types and Functional Group Concentrations <sup>b</sup> as Molar Fractions of Total Organic C													
SBO	Af	NR	OMe	OR	OCO	Ph	PhOH	PhOY	COOM	CON	C=O	Af/Ar	LH
FORSUD	0.43	0.10	0.04	0.10	0.03	0.10	0.02	0.01	0.07	0.09	0.01	3.3	9.3
CVDF	0.31	0.08	0.00	0.20	0.07	0.16	0.06	0.02	0.09	0.01	0.00	1.3	5.3

<sup>a</sup>Concentration values refer to dry matter: the averages and standard deviations calculated over triplicates.

<sup>b</sup>PhOY = alkyl-phenyl ether or diphenyl ether; Af/Ar = Af/(Ph + PhOH + PhOY); lipophilic C = sum of Af, Ph, OMe, CON, NR, RO, PhOY, and OCO C atoms; and hydrophilic C = sum of carboxylate (COOM), PhOH, and C=O C.

definition, LH is an index of the degree of lipophilicity of the SBOs. The other parameter was given by the Af/Ar C ratio, where Ar is the sum of the Ph, PhOY, and PhOH C atoms. By this definition, Af/Ar indicates the type of lipophilicity. Thus, on the basis of the Table II data, we observed that compared to CVDF, FORSUD had the lowest values for the C/N elemental ratio and, for contents of ash and COOH acid groups, exhibited the highest LH and Af/Ar values. This indicated FORSUD as more lipophilic, Af, and with a less acidic product, as characterized by the higher relative content of organic N.

#### Chemical Nature of the EVOH–SBO Films

The SBO are soluble only in water at pH values of greater than 4, whereas EVOH is insoluble in water and soluble in DMSO. The film preparation was, therefore, performed starting from a solution of EVOH in DMSO, to which the aqueous SBO solution was added dropwise while the added water was distilled. In this fashion, several solutions containing SBO and EVOH at a 0.1–0.7 SBO/EVOH weight ratio were made. In all cases, at the end of the SBO addition and after almost all of the added water was distilled, homogeneous solutions were obtained. The addition of water to the previous homogeneous solutions or the addition of an aqueous SBO to the DMSO solution without continuous distillation of the added water resulted in phase inversion with the formation of neat EVOH films and SBO particles dispersed in the mixed DMSO and water solvents. The addition of other solvents immiscible with DMSO, such as cyclohexane, to the homogeneous DMSO solution containing EVOH and SBO did not cause any effect that could be visually appreciated, except the separation of the two solvent layers. These findings suggested the occurrence of reaction 2 (the formation of product I):



In this exemplified reaction,  $n$  is the EVOH/SBO molar ratio and I is the product containing the SBO associated with EVOH molecules by likely proton donor–acceptor interactions. In this way, SBO became soluble in DMSO.

With casting and heating overnight at 105°C, the water-free DMSO solution at a 0.1–0.7 SBO/EVOH weight ratio allowed us to obtain films that, upon washing with water, did not yield complete recovery of the starting reagents. This fact was

assessed by the visual observation of the film water washings and the analysis of the recovered film by spectroscopy, elemental analysis, and potentiometric titration. The water washings of all of the films were colored. This indicated the release of water-soluble SBO material from the cast film. Clear, uncolored water washings were obtained after several washings. The number of water washings required to attain the final uncolored washing depended on the starting SBO/EVOH weight ratio used in the DMSO solution from which the film was cast. The film obtained from the DMSO solution containing neat EVOH was white and transparent. The EVOH–SBO films cast from the DMSO solutions and recovered from the final water washing were also transparent but light or dark brown depending on the starting SBO/EVOH weight ratio. The color of the film recovered from the washing bath was the first indication of the presence of residual water-insoluble SBO firmly bonded to EVOH. The presence of SBO in the washed film was confirmed by IR spectroscopy. Figure 1 shows the IR spectra of the neat reagents used in the preparation of the films and two typical spectra of the films made from EVOH and CVDF and from EVOH and FORSUD. We observed that the spectral region above 2500 cm<sup>-1</sup> was dominated by the broad bands arising from the OH stretching vibration covering the 3600–3000-cm<sup>-1</sup> range and by the bands falling in the 3000–2800-cm<sup>-1</sup> range arising from CH stretching vibrations. These functional groups and C moieties are common to both neat SBO and neat EVOH. On the contrary, the spectral region below 1800 cm<sup>-1</sup> allowed us to distinguish the SBO from EVOH. Indeed, the neat CVDF and neat FORSUD exhibited strong absorptions centered at 1645 and 1573 cm<sup>-1</sup> [Figure 1(e)] and 1651 and 1559 cm<sup>-1</sup> [Figure 1(a)], respectively. These bands arose from the asymmetrical C=O stretching vibrations of carboxylate groups and from the C=O stretching (amide I band) and N–H bending vibrations of CON groups.<sup>16</sup> The presence of these bands was consistent with the functional groups (Table II) identified and determined by <sup>13</sup>C spectroscopy, elemental N analysis, and potentiometric titration. By comparison, the neat EVOH polymer exhibited [Figure 1(c)] its strongest absorption bands centered at 1460, 1334 and 1140, and 1090 cm<sup>-1</sup> arising from the vibrations of the C–C, C–H, and C–OH bonds, respectively, of its molecular structure. The spectra of the EVOH–SBO films exhibited all of the main bands of EVOH and SBO. Typical spectra are reported in Figures 1(b) and 2(d) for the EVOH films containing 5.9% FORSUD and 6.2% CVDF, respectively.

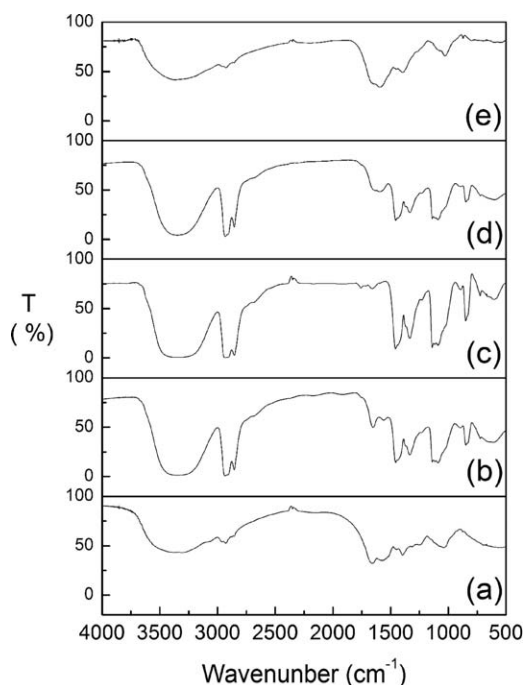


**Figure 1.** FTIR spectra of (a) neat FORSUD, (b) EVOH-5.9% FORSUD, (c) neat EVOH, (d) EVOH-6.2% CVDF, and (e) neat CVDF.

Although IR spectroscopy was useful for assessing the presence of SBO in the films, the determination of the SBO film content was rather difficult. A main problem was the heterogeneity of the SBO molecules. As the C moieties listed in Table II were likely not to be distributed homogeneously over the entire molecular pool, the molecules present in the film might have had a different chemical composition from those leached into the film washing bath. The second problem was that the organic moieties listed in Table II were also composed of Af C atoms and OH functional groups, which were hard to distinguish from those belonging to EVOH. Attempts to solve this problem by spectroscopic techniques were unsuccessful. Under these circumstances, the best way to attempt a quantitative estimate of the SBO film content was through the determination of the films elemental N and COOH functional groups' content. Table III shows data for the SBO organic matter in the EVOH-SBO films calculated (see Experimental section) according to eqs. (1) ( $SBO_{nom1}$ ) and 2 ( $SBO_{nom2}$ ) from the N and COOH analytical values, respectively. We observed that there was fair agreement between  $SBO_{nom1}$  and  $SBO_{nom2}$ . This suggested that the functional groups containing the N and COOH functional groups were homogeneously distributed over the SBO molecules present in the films. On this basis, it was possible to obtain the data shown in Figure 2, which reports the found SBO/EVOH weight ratio in the EVOH-SBO films as a function of the SBO/EVOH weight ratio used in the preparation of the DMSO solution from which the films were cast. We observed that the SBO/EVOH ratio in the film reached a plateau value around 0.25 for CVDF and 0.15 for FORSUD, even when much higher values might have been expected on the basis of the relative composition in the DMSO solution. The higher plateau concentration for CVDF, compared to that of FORSUD, indicated a higher

reactivity of CVDF versus that of EVOH. This may have reflected the different chemical natures of the two SBOs. Table II shows that CVDF had a threefold higher content of PhOH groups than FORSUD. In principle, these groups were capable of reacting with the EVOH hydroxyl groups to yield alkyl-phenyl ether bonds. The reaction of alcohols and PhOHs to yield alkyl-phenyl ethers has been shown to occur under acid-free conditions in aqueous media at moderate temperatures.<sup>17</sup> Thus, it was not unlikely that a condensation reaction between the EVOH hydroxyl functions and the SBO PhOH functional groups occurred during the evaporation of DMSO from the casting solution and the heating of the cast viscous wet layer at 105°C overnight. Reaction 3 (the formation of product II), as follows, is a simplified representation of a condensation reaction between two OH groups belonging to one EVOH and to one SBO molecule. The reaction occurred with the formation of product II, containing the EVOH and SBO molecules bonded through an ether linkage:



Direct evidence of the formation of ether bonds could not be obtained by spectroscopy. The presence of OH functional groups in both the neat EVOH and SBO did not allow us to distinguish the formation of new ether linkages either by IR or <sup>13</sup>C-NMR spectroscopy. Strong indirect evidence in favor of reaction 3 was, however, obtained from studies of the product molar mass and solubility properties.

The molecular characterization of the neat SBO, neat EVOH, and EVOH-SBO films was performed by means of a MALLS absolute detector online to a SEC system. The most important results are shown in Figure 3 and Table I. As shown in Table I, mass recovery from the SEC system ranged from 83 to 97% throughout all of the analyzed samples. Thus, the data reported in Figure 3 and Table I are largely representative of the sample

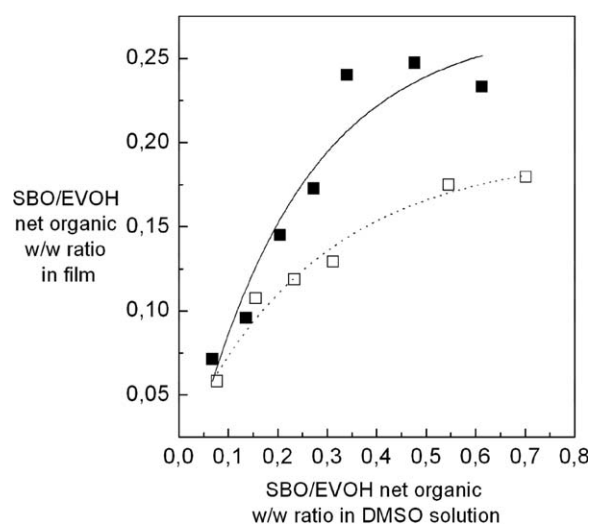


**Figure 2.** Found SBO/EVOH net organic weight ratios in films versus SBO/EVOH net organic weight ratio in DMSO solutions used for the preparation of the EVOH-CVDF films (full symbols and solid line) and EVOH-FORSUD films (open symbols and broken line).

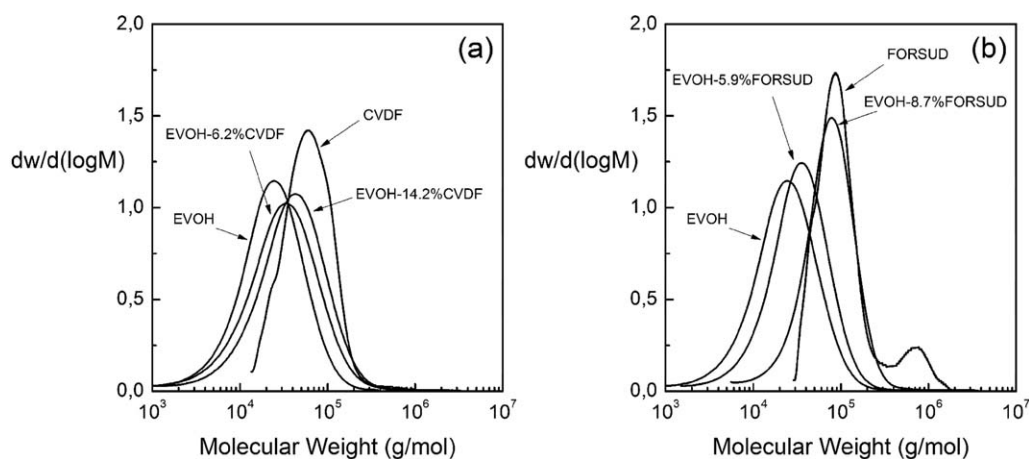
**Table III.** Data for the Neat SBO, EVOH, and EVOH–SBO Films Calculated According to Eqs. (1) and (2)<sup>a</sup>

Sample	N (wt %)	COOH (mol/100 g)	VS (wt %)	SBO <sub>nom1</sub> (wt %)	SBO <sub>nom2</sub> (wt %)
CVDF	5.2	0.279	67.6	—	—
FORSUD	6.6	0.252	77.4	—	—
EVOH	0.0	0.000	99.2	—	—
EVOH–CVDF 0.2 <sup>b</sup>	0.5	0.024	97.4	6.5	5.8
EVOH–CVDF 0.4 <sup>b</sup>	1.1	0.058	95.1	14.3	14.1
EVOH–CVDF 0.7 <sup>b</sup>	1.4	0.081	96.7	18.2	19.6
EVOH–FORSUD 0.2 <sup>b</sup>	0.5	0.020	99.0	5.8	6.1
EVOH–FORSUD 0.4 <sup>b</sup>	0.9	0.030	98.9	10.5	9.2
EVOH–FORSUD 0.7 <sup>b</sup>	0.7	0.030	98.2	8.2	9.2

<sup>a</sup>Concentration with reference to dry matter.<sup>b</sup>SBO/EVOH weight ratio used in the film preparation.

organic matter. Figure 3 shows the differential MWD pattern obtained for the neat EVOH, neat CVDF, neat FORSUD, two EVOH–CVDF products, and two EVOH–FORSUD products. Table I reports the molar masses of the peak of the chromatogram ( $M_p$ ) shown in Figure 3,  $M_w$  values, and the polydispersity index ( $M_w/M_n$ ) values, where  $M_n$  denotes the number-average molar mass. These data add further arguments in favor of reaction 3 between EVOH and SBO. All of the films containing SBOs had rather higher molar masses than one could reasonably expect on the basis of the amount of SBO and on a simple physical mixture of two separate components remaining distinct within a blend structure. Particularly, the EVOH–FORSUD product containing only 5.9% SBO had an  $M_w$  three times greater than that of neat EVOH. Figure 3 shows how the MWD of this film was definitely different from that of neat EVOH and almost overlapped the one of neat FORSUD. Furthermore, the MWDs for this product and for the other EVOH–SBO products were almost symmetrical (not bimodal or multimodal). We could only explain such features by imagining that the small amount of biopolymer molecules reacted to bridge several EVOH molecules and, thus, increased the molar mass of the main polymer in the film.

Treating the films according to Scheme 1 (see Experimental section) allowed us to separate the raw product **II** into a fraction soluble in DMSO (**III**) and a fraction insoluble in DMSO (**IV**). Generally, the amount of **IV** increased with increasing SBO in the raw product **II**. This trend was mostly evident for the EVOH–CVDF films, which according to Figure 1, could be obtained over a wider composition range than for the EVOH–FORSUD films. The data in Figure 4 show that the yield of **IV** increased from 7 to 42% when the CVDF concentration in **II** increased from 7 to 19%. It was also interesting to observe that **III** contained 3–5% CVDF, whereas **IV** contains 34–49% CVDF. These two fractions had rather different behaviors toward aqueous solvents. Fraction **III** was mostly soluble in aqueous DMSO containing up to 70% H<sub>2</sub>O. The amount of insoluble residue in the DMSO–H<sub>2</sub>O solvent (Scheme 1, step 3) was negligible. No chemical composition difference was found between the D (Scheme 1, step 2) and DW recast films (Scheme 1, step 4). Fraction **IV** exhibited the properties of neat SBO; that is, it was mostly soluble in 1M NaOH and precipitated at acid pH. Both fractions were stable upon treatment with alkali. They were recovered nearly quantitatively and were unchanged after 4 h of being kept in 1M NaOH at 60°C. The film stability in 1M

**Figure 3.** (a) Comparison of differential MWDs for EVOH, CVDF, EVOH–6.2% CVDF, and EVOH–14.2% CVDF. (b) Comparison of differential MWDs for EVOH, FORSUD, EVOH–5.9% FORSUD, and EVOH–8.7% FORSUD.

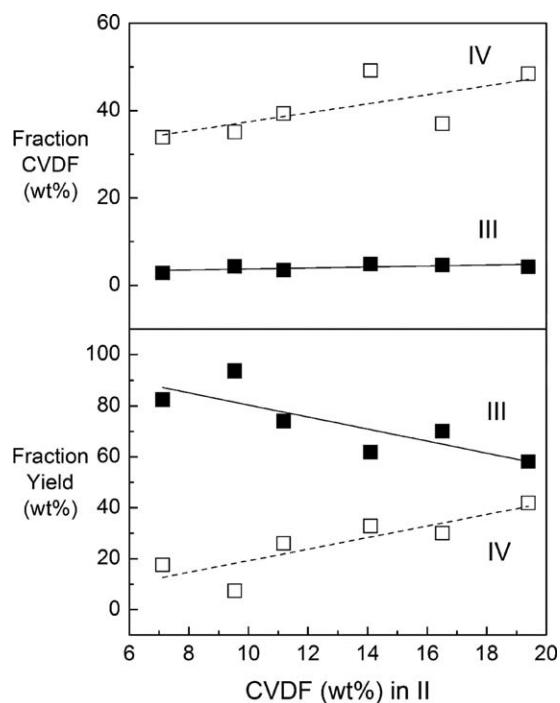


**Figure 4.** Yields and CVDF concentrations in the DMSO-soluble fraction (III) and the DMSO-insoluble fraction (IV) obtained from primary films (II) containing various CVDF concentrations.

NaOH was consistent with the presence of ether linkages bonding EVOH and SBO. To fully appreciate the stability of the chemical bonds between EVOH and SBO, a sample of fraction of III in film form was recycled repeatedly through the alkali treatment. At each cycle, the film was withdrawn from the alkali bath and treated again with fresh 1M NaOH at 60°C for 4 h. The solution was acidified with HCl to yield a precipitate, which was recovered, weighed, and analyzed by IR spectroscopy. This treatment ended when no precipitate was obtained from the alkali bath upon the addition of HCl. Figure 5 reports the amount of materials leached in the alkaline solution from the

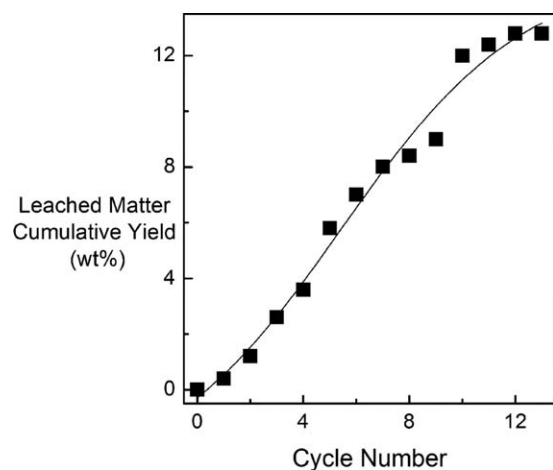


**Figure 5.** Cumulative yields of matter leached in the alkali bath upon the repeated cycling of the EVOH-6.2% CVDF film in fresh 1M NaOH at 60°C for 4 h per cycle.

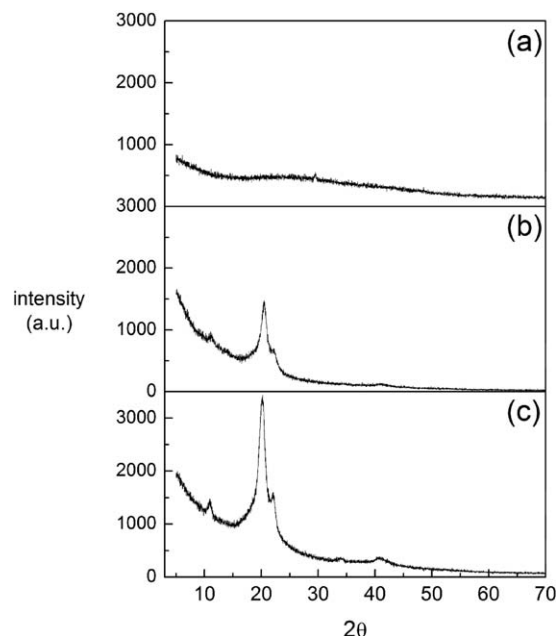


**Figure 6.** XRD patterns of the (a) neat CVDF, (b) neat EVOH, and (c) EVOH-6.2% CVDF cast in the film form.

EVOH film containing 6.2% CVDF. The leached matter precipitated from the alkali bath was found to contain mostly CVDF. No leaching of alkali soluble matter was found in parallel treatments performed with 1M NaOH at room temperature on a different aliquot of the same film.

The results of the Scheme 1 treatments coupled with those of the alkali treatments show that II contained two main fractions, III and IV. Both could be represented with the same general formula for II, where  $n$  decreased in the order III > II > IV. These products had properties ranging from those of neat EVOH to those of neat SBO. Even after strong alkali treatment, the neat components were never obtained. The stability in hot alkali and the change in the solubility properties of the products compared to the neat reagents demonstrated that the materials obtained from EVOH and SBO were not just a physical mixture of the two reagents but were products of a chemical reaction forming covalent stable bonds between the starting reagents molecules. Thus, although product I could be decomposed into the starting reagent by the simple addition of water at room temperature, product II required a strong alkaline treatment to break the chemical bonds between EVOH and SBO and yield products with different EVOH/SBO ratios and solubility properties.

Reaction 3 was found to strongly affect the chemical nature of the starting EVOH polymer. No glass transition or melting up to 220°C was evidenced by DSC for neat SBO. At this temperature, both CVDF and FORSUD started to decompose. On the contrary, the neat EVOH and the EVOH-SBO films exhibited glass-phase transition and melting. XRD analysis showed that the neat SBO was mostly amorphous, whereas the neat EVOH and the EVOH-SBO films exhibited some crystallinity. Figure 6 shows selected typical XRD patterns for neat CVDF and for the neat EVOH and EVOH-6% CVDF films. The melting enthalpy



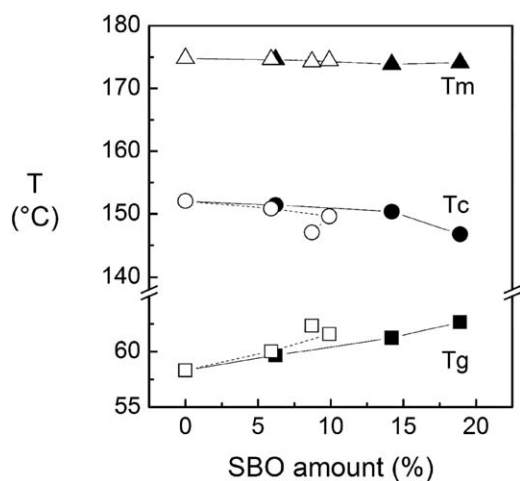


**Figure 7.** Trends of glass transition temperature  $T_g$ , melting temperature  $T_m$  and crystallization temperature  $T_c$  as a function of the amount of CVDF (full symbols) or FORSUD (open symbols).

( $\Delta H_m$ ) and recrystallization enthalpies measured from the DSC scans were found to decrease with increasing SBO concentration in the film. Table I reports typical  $\Delta H_m$  values measured for the EVOH–SBO films compared to those of neat EVOH. The data allowed the calculation of the concentration of the crystalline (EVOH<sub>c</sub>) fraction of the synthetic polymer and of the amorphous (EVOH<sub>nm</sub>) fraction according to eqs. (3)–(5). Similar enthalpy changes were reported for EVOH/copolyamide 6/6.9<sup>18</sup> and EVOH/polyamide blends.<sup>19</sup> Figure 7 shows the glass-transition temperature ( $T_g$ ) and melting temperature ( $T_m$ ) values upon heating at 10  $^{\circ}\text{C}/\text{min}$  and the recrystallization temperature ( $T_c$ ) upon cooling at the same rate as a function of the EVOH–CVDF and EVOH–FORSUD chemical compositions. The results show that with increasing concentration of SBO (either CVDF or FORSUD) and/or of the amorphous fraction of the synthetic polymer, the film  $\Delta H_m$  decreased, no change in  $T_m$  occurred,  $T_g$  increased, and  $T_c$  decreased.

### Film Mechanical Behavior

All of the films had mechanical consistency, which allowed their handling and bending at a 180  $^{\circ}$  angle without breaking, except for the films containing CVDF at concentrations of 19% or greater; these were brittle and fragile. Figure 8 shows, as a representative example, the shear storage modulus ( $G'$ ), loss modulus ( $G''$ ), and loss tangent ( $\tan \delta$ ) as a function of  $\omega$  for the EVOH films containing different amounts of CVDF. The same behavior was observed for the samples containing different amounts of FORSUD. The viscoelastic behaviors of the neat EVOH and EVOH–SBO films were different. At low  $\omega$ , the virgin EVOH seemed to obey linear viscoelasticity model predictions,<sup>20,21</sup> according to which the  $G'$  results were proportional to  $\omega^2$  (curves with slope 2 in Figure 8) and  $G''$  to  $\omega$  (curves with slope 1 in Figure 8). In contrast, a more complex behavior was seen for the EVOH–CVDF product, in which the  $G'$  versus  $\omega$  slope (Figure 9) decreased in the low- $\omega$  region as the SBO amount increased. These results were in agreement with those reported for other blends systems.<sup>21–23</sup> Whether the slope of  $\log G'$  as a function of  $\log \omega$  at low  $\omega$  is close to 2 or lower than 2

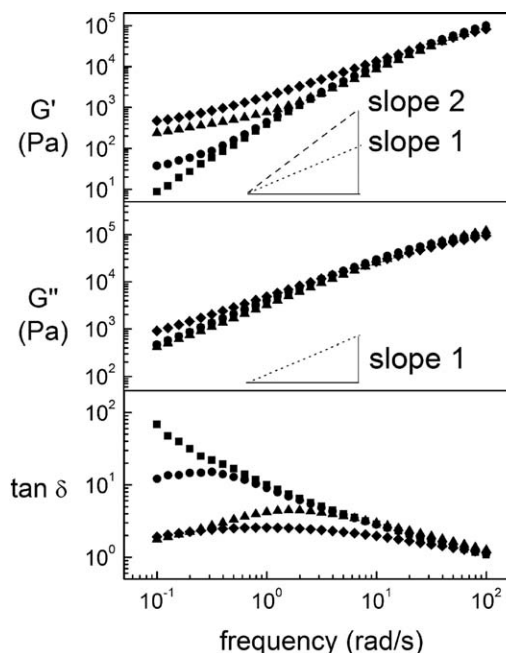


**Figure 8.** Trends of  $G'$ ,  $G''$ , and  $\tan \delta$  values as a function of  $\omega$  for the (■) neat EVOH and EVOH films containing (●) 6.2, (▲) 14.2, and (◆) 18.9% CVDF.

could be used as a criterion for assessing whether a homogeneous (or heterogeneous) structure in a multicomponent polymer system exists. The decrease in the slope of  $\log G'$  versus  $\log \omega$  in the low- $\omega$  region is often correlated to the emergence of phase separation<sup>24</sup> or the presence of various structures, such as agglomerations<sup>25</sup> and networks.<sup>26</sup> The rheological behavior of the EVOH–CVDF and EVOH–FORSUD systems clearly pointed out the heterogeneous nature of these blends; this was in full agreement with the results of the thermal and chemical characterizations.

The EVOH–SBO films were subjected to a stress–strain analysis at a 0.01  $\text{s}^{-1}$  strain rate to investigate the effect of the SBO

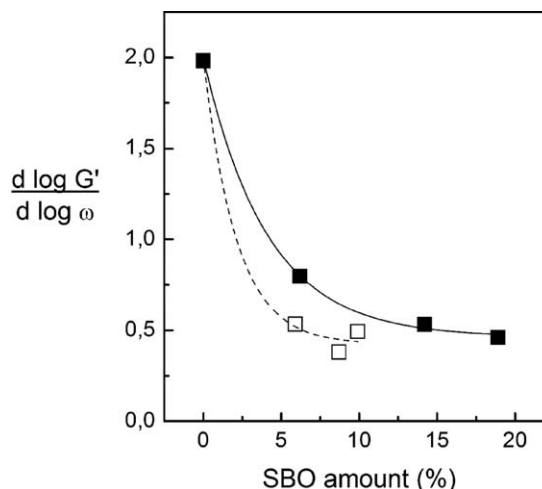


**Figure 9.** Slope of the  $G'$ – $\omega$  curve in the low- $\omega$  region of Figure 8 as a function of the SBO concentration for (■) EVOH–CVDF and (□) EVOH–FORSUD films.

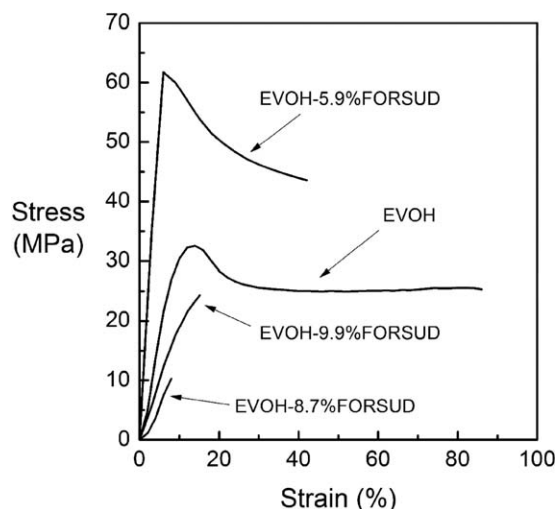


**Figure 10.** Stress–strain curves of the neat EVOH and EVOH films containing FORSUD with the compositions reported in Table I.

addition on the modulus and its ultimate mechanical properties. Figure 10 reports the stress–strain curves for the EVOH–FORSUD films (Table I) compared to the neat EVOH film. The strain at break and Young's modulus values of the neat EVOH film were 86.2%, and 352 MPa, respectively; these were in agreement with the literature.<sup>27</sup> By comparison, the film containing 5.9% FORSUD and characterized by the highest molar mass (Table I) exhibited the highest Young's modulus (1082 MPa) and a decrease in the strain at break to 42.3%. At higher FORSUD amounts, the Young's modulus and strain at break values were lower than those of the neat EVOH. Similar changes in the mechanical behavior as a function of the SBO concentration were observed for the EVOH–CVDF films. The film made from the raw product II containing 7.1% CVDF (Figure 4) exhibited a Young's modulus equal to that of the pure EVOH but a higher stress at yield and a lower strain at break. All of other films containing higher CVDF concentrations exhibited very poor

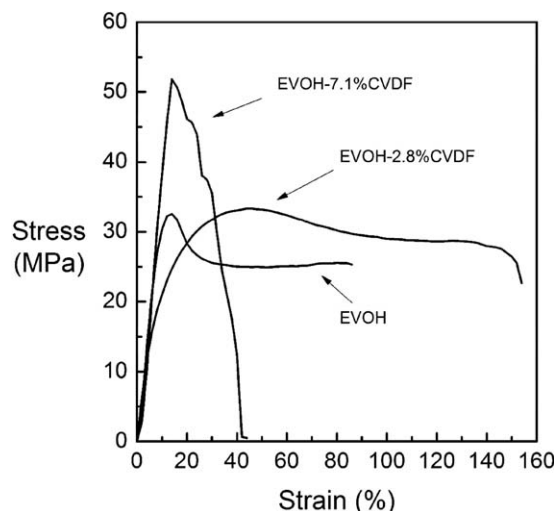


**Figure 11.** Stress–strain curves of the neat EVOH and EVOH films (Table I) made from II and containing 7.1% CVDF and from III containing 2.8% CVDF.

mechanical properties. However, when the film was dissolved in DMSO, separated from the insoluble fraction, and recast (see Scheme 1, step 2, D recast films), a new film containing 2.8% CVDF was obtained. The stress–strain curve of this latter film is compared in Figure 11 to the neat EVOH film and to the original product containing 7.1% CVDF. It was apparent that the recast film exhibited a Young's modulus comparable to that of the pure EVOH and a substantially higher strain at break.

### SBO Effects' Dependence on the Concentration and Chemical Nature

All together, the results show that the SBOs were high-molecular-weight biopolymers that modified the thermal, rheological, and mechanical properties of the starting synthetic polymer. Similar effects are reported in the literature for blends made from PVA and natural materials, such as algae,<sup>28</sup> corn fiber,<sup>5</sup> hyaluronic acid,<sup>29,30</sup> and sugar cane bagasse.<sup>6</sup> We determined in this study that the SBOs increased the yield strength of the synthetic polymer when present at low concentrations (ca. 6–7%). At higher SBO concentrations, the mechanical properties of the film deteriorated greatly. The results show that compared to the EVOH–5.9% FORSUD film (Figure 9), the EVOH–7.1% CVDF film (Figure 10) exhibited over 30% lower stress at the yield point. Thus, although both SBOs induced the strengthening of the neat EVOH film when present at low concentrations, FORSUD was more effective. The chemical data available for the two SBOs (Table II) showed that these two materials were different in the degree of hydrophilicity (LH) and the ratio of Af to aromatic C (Af/Ar). The chemical differences were apparently connected to the different mechanical strengthening effects shown previously. The results offer scope for further development work on these materials and investigation on SBOs sourced from other biowastes to better understand the reasons for the observed effects and to exploit their full potential to modify synthetic polymers.

### CONCLUSIONS

New materials were obtained from a synthetic polymer with hydroxyl functional groups (EVOH) and biopolymers (SBO) with acid and basic functional groups. Evidence was provided for a condensation reaction occurring between EVOH and SBOs and yielding products in which the biopolymer was covalently bonded to the synthetic polymer. These products had higher molecular weights and different thermal, rheological, and mechanical behaviors compared to the starting synthetic polymer. The properties of the blended films were found to be dependent of the chemical nature and relative content of the biopolymers. Worthwhile research scopes are possible for the development of new materials containing biopolymers isolated from wastes.

### ACKNOWLEDGMENTS

This work was performed with funds from the Ministero delle Politiche Agricole e Forestali for the Agrienergia project. The authors are grateful to the following private and/or public Italian institutions: Acea Pinerolese Spa in Pinerolo (Turin) for supplying the SBO sourcing materials and Studio Chiono ed Associati in

Rivarolo Canavese for making available pilot equipment and services for the production of the SBO.

## REFERENCES

1. Montoneri, E.; Boffa, V.; Savarino, P.; Perrone, D. G.; Montoneri, C.; Mendichi, R.; Acosta, E. J.; Kiran, S. *Biomacromolecules* **2010**, *11*, 3036.
2. Bastioli, C.; Bellotti, V.; Del Giudice, L.; Gilli, G. *J. Environ. Polym. Degrad.* **1993**, *1*, 181.
3. Ismail, H.; Zaaba, N. F. *J. Vinyl Addit. Technol.* **2014**, *20*, 72.
4. Zhou, X. Y.; Jia, D. M.; Xie, D. *J. Reinf. Plast. Compos.* **2009**, *28*, 2771.
5. Cinelli, P.; Chiellini, E.; Lawton, J. W.; Imam, S. H. *J. Polym. Res.* **2005**, *13*, 107.
6. Chiellini, E.; Cinelli, P.; Solaro, R.; Laus, M. *J. Appl. Polym. Sci.* **2003**, *92*, 426.
7. Ramaraj, B. *J. Appl. Polym. Sci.* **2007**, *106*, 1048.
8. Ramaraj, B. *J. Appl. Polym. Sci.* **2007**, *103*, 1127.
9. Pua, F. L.; Sapuan, S. M.; Zainudin, E. S.; Adib, M. Z. *J. Biobased Mater. Bioenergy* **2013**, *7*, 95.
10. Sheldon-Coulson, G. A. Production of Levulinic Acid in Urban Biorefineries; Massachusetts Institute of Technology Libraries: Cambridge, MA, **2011**.
11. Montoneri, E.; Mainero, D.; Boffa, V.; Perrone, D. G.; Montoneri, C. *Int. J. Global Environ.* **2011**, *11*, 170.
12. Mendichi, R.; Giacometti Schieroni, A. *Curr. Trends Polym. Sci.* **2001**, *6*, 17.
13. Wyatt, P. *J. Anal. Chim. Acta* **1993**, *272*, 1.
14. Mauro, N.; Manfredi, A.; Ranucci, E.; Procacci, P.; Laus, M.; Antonioli, D.; Mantovani, C.; Magnaghi, V.; Ferruti, P. *Macromol. Biosci.* **2013**, *13*, 332.
15. Renò, F.; Carniato, F.; Rizzi, M.; Marchese, L.; Laus, M.; Antonioli, D. *J. Appl. Polym. Sci.* **2013**, *129*, 699.
16. Silverstein, R. M.; Webster, F. X.; Kiemle, D. J. Spectrometric Identification of Organic Compounds; Wiley: New York, **1997**.
17. Reddy, K. R.; Rajanna, K. C.; Ramgopal, S.; Kumar, M. S. *Green Sustainable Chem.* **2012**, *2012*, 123.
18. Nir, Y.; Narkis, M.; Siegmann, A. *Polym. Eng. Sci.* **1998**, *3*, 1890.
19. Lagaron, J. M.; Gimenez, E.; Saura, J. J.; Gavara, R. *Polymer* **2001**, *42*, 7381.
20. Ferry, J. D. Viscoelastic Properties of Polymers; Wiley: New York, **1980**.
21. Haley, J. C.; Lodge, T. P. *J. Rheol.* **2004**, *48*, 463.
22. Han, C. D.; Chuang, H.-C. *J. Appl. Polym. Sci.* **1985**, *30*, 4431.
23. Han, C. D.; Yang, H. H. *J. Appl. Polym. Sci.* **1987**, *33*, 1199.
24. Zheng, Q.; Du, M.; Yang, B.; Wu, G. *Polymer* **2001**, *42*, 5743.
25. Wu, G.; Zheng, Q. *J. Polym. Sci. Part B Polym. Phys.* **2003**, *42*, 1199.
26. Hu, G.; Zhao, C.; Zhang, S.; Yang, M.; Wang, Z. *Polymer* **2006**, *47*, 480.
27. Cabedo, L.; Lagarón, J. M.; Cava, D.; Saura, J. J.; Giménez, E. *Polym. Test.* **2006**, *25*, 860.
28. Chiellini, E.; Cinelli, P.; Ilieva, V. I.; Martera, M. *Biomacromolecules* **2008**, *9*, 1007.
29. Lazzeri, L.; Barbani, N.; Cascone, M. G.; Lupinacci, D.; Giusti, G.; Laus, M. *J. Mater. Sci.: Mater. Med.* **1994**, *5*, 862.
30. Ramires, P. A.; Milella, E. *J. Mater. Sci.: Mater. Med.* **2002**, *13*, 119.